EAST EUROPEAN JOURNAL OF PHYSICS. 1. 82-88 (2023)
DOI:10.26565/2312-4334-2023-1-09 ISSN 2312-4334

THEORETICAL STUDY OF MATTER DENSITY DISTRIBUTIONS, AND ELASTIC ELECTRON SCATTERING FORM FACTORS OF EXOTIC NUCLEI (^{26}F AND ^{9}C)†

Abeer A. M. Hussein*, Ghaith N. Flaiyh
Department of Physics, College of Science, University of Baghdad, Baghdad, Iraq
**Corresponding Author e-mail: Abeer.Ali1104a@sc.uobaghdad.edu.iq*
Received November 30, 2022; revised December 23, 2022; accepted December 26, 2022

The distributions of nuclear density, root mean square radii, and elastic electron scattering form factor are calculated for nuclei (^{9}C) (core +2p) and (^{26}F) (core +2n) with the two different nuclear potential parameters for (*bc*) and (*bv*), where correlations for both the (effects tensor force and short-range) are used, and the appearance of the long extension is observed in nuclear density distributions for these nuclei. Fortran 95 power station was used to program nuclear properties such as nucleon density (matter, neutron, and proton), elastic electron scattering form factor, and *rms* radii. The computed results for these exotic nuclei are determined to correspond pretty well with the experimental data.
Keywords: *Exotic nuclei; Form factor; Nuclear density (neutron, proton, matter); Neutron-rich; Proton-rich*
PACS: 21.10k, 21.10ft, 21.10Gv, 21.60Jz, 25.40.-h, 25.40.Cm, 25.40.Dn

1. INTRODUCTION

From properties the Halo nuclei: a few weakly bound halo nucleons and a more strongly bound core where This scale separation can be exploited in a few-body description of halo nuclei, because the halo nucleons do not determine the exact structure of the core [1]. Nuclear density distribution is an important factor [2] it's an essential component of both experimental and theoretical research, where the experimental matter density distributions of unusual nuclei are characterized mostly by long tail behavior [3]. Numerous solutions have been put out to deal with tension forces since including short-range correlations and tension forces is a difficult challenge, particularly for the theory of nuclear structure [4,5]. Dellagiacoma et al. presented a simple phenomenological strategy for establishing dynamic short-range and tensor effects [6].

The neutron halo in some neutron-rich nuclei is one of the most intriguing discoveries in recent experimental research employing radioactive nuclear beams [7,8]. Halo nuclei (^{8}He and ^{26}F) were studied by Ghufran M. [9] using the 3-body harmonic oscillator model and Woods-Saxon radial wave functions. While studying the theoretical outlines of calculations, assume that the nuclei understudy are composed of two parts: the stable core and the unstable halo, where the core part is studied using the radial wave functions of harmonic-oscillator (HO) potentials, and the halo is studied using the Woods-Saxon (WS) potential for (^{8}B, ^{17}Ne, ^{11}Be, and ^{11}Li) nuclei by Arkan et al. [10].

In contrast, research on the proton halo in proton-rich nuclei has piqued the curiosity of many in last years, with theory based on relative mean approximation (RMF) predicting the presence of a proton halo structure in some proton-rich nuclei [11, 12], and The ground-state density of the unstable proton-rich ^{9}C, ^{12}N, and ^{23}Al exotic nuclei was investigated using the dual-frequency shell model and binary mass model [13]. The proton emission potentials of several single protons and proton halo nuclei of heavy isotopes (SH) with Z= 121–128 were investigated using the Coulomb model and the proximity potentials as a reactive barrier by Anjali. and others [14].

In this work are studied using the formula two-body charge density distributions for the halo nuclei {^{26}F(core+2n)} and {^{9}C(core+2p)} by using two function shell model (TFSM) with two different parameters *bc* and *bv* for calculated The root mean square radii (*rms*), form factors and the nuclear density (matter, protons, and neutrons) of the ground state with full correlation effects (short range and tensor force).

2. THEORY

The following transforms the one-body density in eq. (1) operator into a two-body density form $\hat{\rho}^{(1)}(\vec{r}) \Rightarrow \hat{\rho}^{(2)}(\vec{r})$ as shown in eq. (2) [15]:

$$\hat{\rho}^{(1)}(\vec{r}) = \sum_{i=1}^{A} \delta(\vec{r} - \vec{r}_i) \tag{1}$$

$$\sum_{i=1}^{A} \delta(\vec{r} - \vec{r}_i) \equiv \frac{1}{2(A-1)} \sum_{i \neq j} \left\{ \delta(\vec{r} - \vec{r}_i) + \delta(\vec{r} - \vec{r}_j) \right\} \tag{2}$$

Another relevant transformation is that of the coordinates of the two particles, which may be expressed, ($\vec{r}_i$ and $\vec{r}_j$), in terms of that relative $\vec{r}_{ij}$, and center -of- mass $\vec{R}_{ij}$ coordinates [16]:

† ***Cite as:*** A.A.M. Hussein, and G.N. Flaiyh, East Eur. J. Phys. **1**, 82 (2023), https://doi.org/10.26565/2312-4334-2023-1-09

$$\vec{r}_{ij}=\frac{1}{\sqrt{2}}(\vec{r}_i-\vec{r}_j) \tag{i}$$

$$\vec{R}_{ij}=\frac{1}{\sqrt{2}}(\vec{r}_i+\vec{r}_j) \tag{ii}$$

Using Eqs. (i) and (ii) in Eq. (2)

$$\hat{\rho}^{(2)}(\vec{r})=\frac{1}{2(A-1)}\sum_{i\neq j}\left\{\delta\left[\vec{r}-\frac{1}{\sqrt{2}}(\vec{R}_{ij}+\vec{r}_{ij})\right]+\delta\left[\vec{r}-\frac{1}{\sqrt{2}}(\vec{R}_{ij}-\vec{r}_{ij})\right]\right\} \tag{3}$$

Using the identity by Hamoudi et al. [17] $\delta(a\vec{r})=\frac{1}{|a^3|}\delta(\vec{r})$ (for three-dimension)

Where (a), is a constant. Then eq. (3) becomes:

$$\hat{\rho}^{(2)}(\vec{r})=\frac{\sqrt{2}}{(A-1)}\sum_{i\neq j}\left\{\delta\left[\sqrt{2}\vec{r}-\vec{R}_{ij}-\vec{r}_{ij}\right]+\delta\left[\sqrt{2}\vec{r}-\vec{R}_{ij}+\vec{r}_{ij}\right]\right\} \tag{4}$$

The operator from Equation (4), can be folded with the two-body operator functions $\tilde{f}_{ij}$ to yield an efficient two-body charge density operator, (utilized for uncorrelated wave functions).

$$\hat{\rho}^{(2)}_{eff}(\vec{r})=\frac{\sqrt{2}}{(A-1)}\sum_{i\neq j}\tilde{f}_{ij}\left\{\delta\left[\sqrt{2}\vec{r}-\vec{R}_{ij}-\vec{r}_{ij}\right]+\delta\left[\sqrt{2}\vec{r}-\vec{R}_{ij}+\vec{r}_{ij}\right]\right\}\tilde{f}_{ij} \tag{5}$$

Where the from $\tilde{f}_{ij}$, is given by [18]

$$\tilde{f}_{ij}=f(r_{ij})\Delta_1+f(r_{ij})\left\{\ 1+\alpha(\mathrm{A})B_{ij}\ \right\}\Delta_2 \tag{6}$$

It's evident of eq. (6), includes two kinds of effects:

I. The first term of equation (6), two-body short range correlations, denoted by (r_{ij}). Here Is a projection operator on the space of all two-body wave functions, with the exception of $^3S^1$ and $^3D_1$ states. Short-range correlations are significant functions of particle separation because they reduce the two-body wave function at short distances where the repulsive core drives the particles apart and heal to unity at long distances where the interactions are very weak. [19] gives the two-body short range correlation**.**

$$f(r_{ij})=\begin{Bmatrix}0 & for\ r_{ij}\le r_c\\ 1-\exp\{-\mu(r_{ij}-r_c)^2\} & for\ r_{ij}>r_c\end{Bmatrix} \tag{7}$$

II. When r_c (*fm*), is the radius of a suitable hard core, and μ =25 fm^{-2} [18], correlation parameter.

The strong tensor, component in the nucleon - nucleon force induces the longer range two- body tensor correlations, that are shown in the second term of equation (6). This projection operator only affects the $^3S_1$ and $^3D_1$ states. The typical tensor operator, B_{ij}, is known as [18], and is created by the scalar product for intrinsic spin space, with coordinate space:

$$B_{ij}=\frac{3}{r_{ij}^2}(\vec{\sigma}_i.\vec{r}_{ij})(\vec{\sigma}_j.\vec{r}_{ij})-\vec{\sigma}_i.\vec{\sigma}_j \tag{8}$$

It makes sense to parameterize the core, and halo densities independently in the case of exotic (halo) nuclei. Eq. (5)'s ground state density distribution can be separated into two portions, one of which is the matter density distribution for the complete exotic nucleus [20].

$$\rho_m(r)=\rho^c_{(p+n)}(r)+\rho^v_n(r) \tag{9}$$

The following formulas produce the *rms* radii of the matching aforementioned densities [20]:

$$\left\langle r^2\right\rangle^{1/2}_U=\frac{4\pi}{U}\int_0^\infty\rho^U(r)r^4\,dr \tag{10}$$

Where U is (proton, neutron or matter). Using ground-state charge density distributions, the elastic electron scattering form factor can be computed. According to the Plane Wave Born Approximation (PWBA), incident and dispersed electron waves are assumed to be plane waves, and charge density distributions are real and spherical symmetric, therefore the form factor is just the Fourier transform of the charge density distribution, resulting in [21]:

$$F(q)=\frac{4\pi}{qZ}\int_0^{\infty}\rho_o(\mathrm{r})\mathrm{Sin}(q\mathrm{r})\mathrm{r}\;dr\,F_{fs}(q)\,F_{cm}(q) \tag{11}$$

Where $F_{cm}(q)$, is the center of mass corrections and F_{fs} (q), is the finite nucleon size The free nucleon form factor, $F_{fs}(q)$ is considered to be the same for protons and neutrons. This correction is written as follows [21]:

$$F_{fs}(q)=e^{-0.43q^2/4} \tag{12}$$

Where the free nucleon form factor F_{fs} (q), for protons and neutrons is consider to be the same. According to [20], the center of mass correction F_{cm} (q) is as follows:

$$F_{cm}(q)=e^{q^2w^2/4A} \tag{13}$$

Where (w) is the harmonic-oscillator size parameter, and (A) is the nuclear mass number.

As a result, when the shell model wave function is, removes F_{cm} (q) eliminates the spurious state caused by the center of mass's motion. The ground state (r) of equation (5), which we obtain after these modifications, can now be used to calculated the form factor $F(q)$ incorporating the impact of two- body correlation functions (11).

3. RESULTS AND DISCUSSION

The nuclear ground state properties of two-neutron (^{26}F) and two-proton (^{9}C) exotic nuclei have been calculated using two- body nucleon density distributions, with including the effect of two-body correlations tenser force (α=0.1) and short range (rc=0.5 fm) using two frequency shell model (TFSM) by relying on equations 5, 7, and 8, where the two particle harmonic oscillator wave functions were employed with two different size parameters of b_c and b_v, where we supposed that which the two- neutron occupies the $2s_{1/2}$ orbital for (^{26}F) and two- proton occupies the $1p_{1/2}$ for (^{9}C) . Elastic electron scattering form factors for these nuclei are studied through combining the charge density distribution with the Plane Wave Born Approximation.

Table 1 Show average radius of neutrons and protons was calculated based on equations (5), (6) and (10), where we got the results when the full correlation (r_c=0.5 fm, α =0.1) and without correlation (r_c=0, α=0) .

Table 2 displays the values of the harmonic oscillator size parameter b_c and b_v utilized in the two function shell model (TFSM) of the present calculations for the selected exotic nuclei and the calculated *rms* radii for core (^{24}F and ^{7}Be) nuclei and exotic nuclei (^{26}F and ^{9}C) when FC's (r_c = 0.5 fm, α = 0.1) the calculated results are in good agreement with the indicated experimental data [22, 23, 24].

Table 1. The computed neutron and proton *rms* radii for (^{26}Fand ^{9}C) nuclei.

Exotic nuclei ^{26}F			
Proton size parameter	**b_p=1.965 fm**	**Neutron size parameter**	**b_n=2.09 fm**
$\langle r_p^2\rangle^{1/2}_{r_c=0.5,\alpha=0.1}$	**2.955663**	$\langle r_n^2\rangle^{1/2}_{r_c=0.5,\alpha=0.1}$	**3.512850**
$\langle r_p^2\rangle^{1/2}_{r_c=0,\alpha=0}$	**2.955916**	$\langle r_n^2\rangle^{1/2}_{r_c=0,\alpha=0}$	**3.525076**
$\langle r_p^2\rangle^{1/2}_{exp}$ [23]	**2.95**	$\langle r_n^2\rangle^{1/2}_{exp}$ [23]	**3.53±0.17**
$\langle r_p^2\rangle^{1/2}_{FC's}$	**-0.0002**	$\langle r_n^2\rangle^{1/2}_{FC's}$	**-0.012**
Exotic nuclei ^{9}C			
Proton size parameter	**b_p=1.85 fm**	**Neutron size parameter**	**b_n=1.77fm**
$\langle r_p^2\rangle^{1/2}_{r_c=0.5,\alpha=0.1}$	**2.681358**	$\langle r_n^2\rangle^{1/2}_{r_c=0.5,\alpha=0.1}$	**2.258469**
$\langle r_p^2\rangle^{1/2}_{r_c=0,\alpha=0}$	**2.677457**	$\langle r_n^2\rangle^{1/2}_{r_c=0,\alpha=0}$	**2.242334**
$\langle r_p^2\rangle^{1/2}_{exp}$ [24]	**2.684**	$\langle r_n^2\rangle^{1/2}_{exp}$	**-**
$\langle r_p^2\rangle^{1/2}_{FC's}$	**-0.003**	$\langle r_n^2\rangle^{1/2}_{FC's}$	**-0.016**

Table 2. bc and bv parameters used in the current study's two function shell model (TFSM), in addition to computed and experimental data rms radii of ^{26}F and ^{9}C halo nuclei.

Halo nuclei	**Core nuclei**	**b_c (fm)**	**b_v (fm)**	**b_m (fm)**	***rms* matter radii for core nuclei $\langle r^2\rangle_c^{1/2}$ (fm)**		***rms* matter radii for halo nuclei $\langle r^2\rangle_m^{1/2}$ (fm)**	
					Calculated results	Experimental Data	Calculated results	Experimental Data
^{26}F	**^{24}F**	1.93	3.649	2.025	3.028205	3.03 ± 0.06 [22]	3.23719	3.23 ± 0.13 [23]
^{9}C	**^{7}Be**	1.76	3.47	1.78	2.311942	2.31 ± 0.02 [24]	2.422160	2.42 ± 0.03 [24]

A. Exotic nuclei ^{26}F

The nucleus ^{26}F is the first observed case of a neutron halo in 1979, and is unstable with respect to β-decay, with a half-life time ($\tau_{1/2}$ =8.2 *ms*) and neutron separation energy (S_{2n} = 5.04 *MeV*). The halo nucleus ^{26}F (J^{π},T =1^{+},4) is formed by coupling the core ^{24}F (J^{π} ,T= 3^{+},3) with the valence (halo) two neutron (J^{π} ,T=0^{+},1) [25-26]. The blue curve represents 2BNDD's for the core nuclei ^{24}F (proton + neutron) with oscillator size parameter (b_c =1.93 *fm*). The green curve represents 2BNDD's for valence (two neutrons) for ^{26}F nuclei with oscillator size parameter (b_v=3.649 *fm*), while the red solid curve represents the total calculation for the core nucleons and the valence two neutrons, and the shaded curve represents the experimental of nucleon densities of ^{26}F [23]. Figure (1) shows the computed matter density distributions show long tail for all of these nuclei and shows that the halo phenomenon and the long tail in ^{26}F is connected to the outer two neutrons for nucleon densities but not to the core nucleons, which is consistent with the experimental data [23], we have a long tail that agrees with the experimental data.

Figure (2) illustrates a calculated of the matter density distributions of neutron-rich ^{26}F (red curve) with the matter density distributions of the stable nuclei ^{19}F (yellow curve) by using two –body charge density distributions with effect of short range (r_c= 0.5*fm*) and tensor force (α = 0.1), we shown along tail is clearly in the matter distribution of the halo nuclei.

The neutron (blue curve), proton (brown curve), and matter (red curve) show densities of ^{26}F we show in Figure (3).

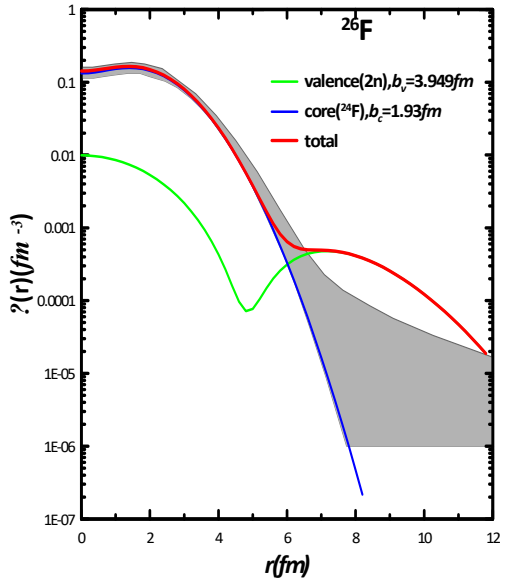

Figure 1. Core, valence and matter density distributions of (^{26}F)

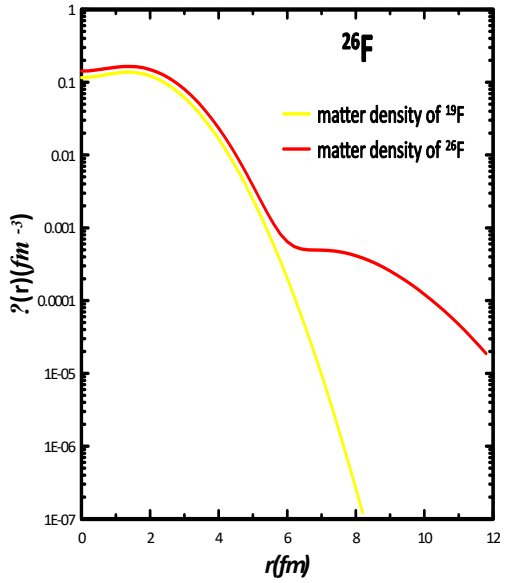

Figure 2. Calculated matter density distribution of neutron-rich (^{26} F) with that of stable nuclei (^{19}F)

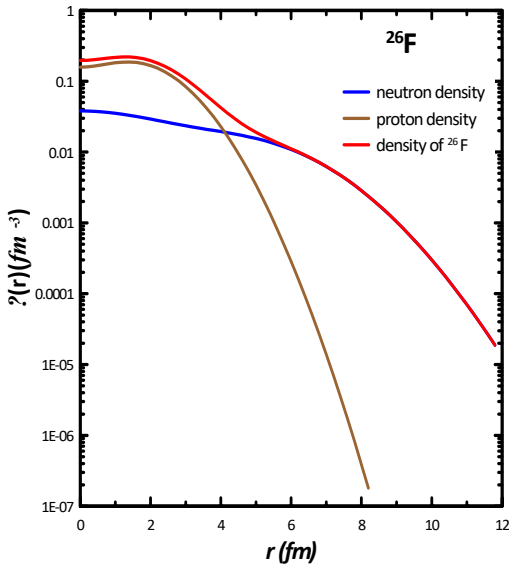

Figure3. Proton, neutron, and matter densities were calculated for ^{26}F halo nuclei

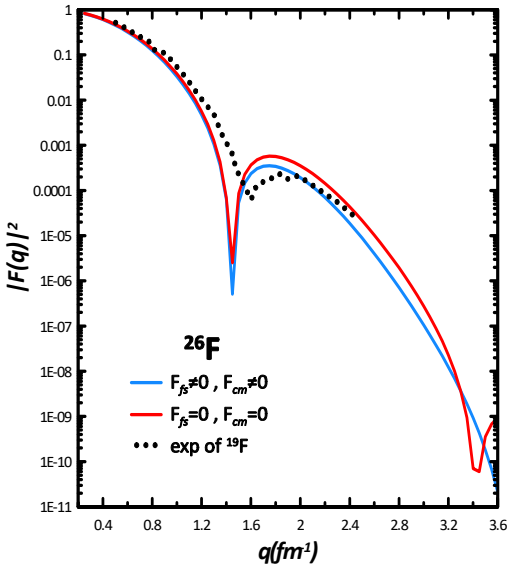

Figure 4. Elastic scattering electron form factor for ^{26}F with experimental data [27].

The neutron *rms* radius is found to be more than the proton *rms* radius, the neutron diffuseness is greater than the proton diffuseness in ^{26}F, and there is a considerable density differential between neutron and proton in ^{26}F, The typical behavior of the halo nucleus (the long tail) is clearly seen in the two neutron for ^{26}F distributions (blue curve), as shown in these figure. We note that the difference between the radii of the neutron and the proton is (r_n-r_p= 0.5571 *fm*) for ^{26}F. This difference is also supported by the halo structure for these alien cores.

Figure (4) presents the electron form factor for ^{26}F with FC'S using PWBA. Where the average radii of nuclei (b=2.025*fm*) were used, these values were adopted by comparing $\langle r^2 \rangle_{\exp}^{1/2}$ with $\langle r^2 \rangle_{the}^{1/2}$ we get a match with the experimental data. The blue curve represents the form factor of 2BCDD's with finite nucleon size corrected and center of mass correction ($F_{fs}(q) \neq 0$,$F_{cm}(q) \neq 0$) , the red curve represents the form factor of 2BCDD's with ($F_{fs}(q)$=0 , $F_{cm}(q)$=0) and the circle-packed are experimental data for stable nuclei ^{19}F [27]. We obtain the Form factors are not dependent on the neutrons that make up the halo but rather results from a difference in the proton density distribution of the last proton in the nuclei, obtain good form factors at the momentum for q<3.6 *fm* and we note that the behavior of the theoretical results for halo nuclei (^{26}F) matches the practical results for stable nuclei (^{19}F).

B. Exotic nuclei ^{9}C

The proton-halo nucleus ^{9}C is an interesting candidate with ($\tau_{1/2}$=126.5 *ms*) for studying the existence of two-proton halo because of the borromean structure and small two-proton separation energy (S_{2p}= 1.436 *MeV*) [25, 26]. ^{9}C (J^{π},T= 3/2, 3/2) is composed of a core ^{7}Be ($J^{\pi}, T = 3/2^{-}$, 3/2) with ($\tau_{1/2}$=53.22 *d*) and outer two loosely bound protons (J^{π}, $T = 0^{+}$, 1) surrounding the core to form the ^{9}C nucleus halo.

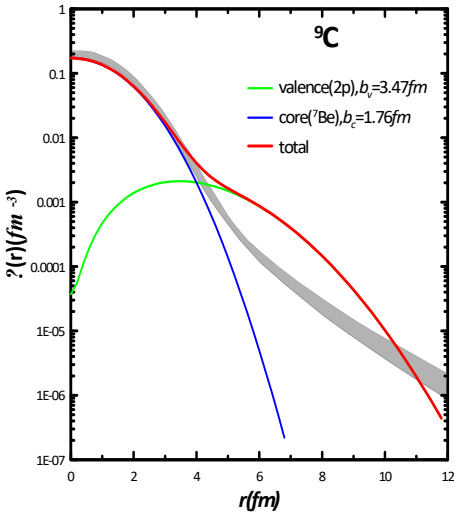

Figure 5. Core, halo and matter density distribution of (^{9}C)

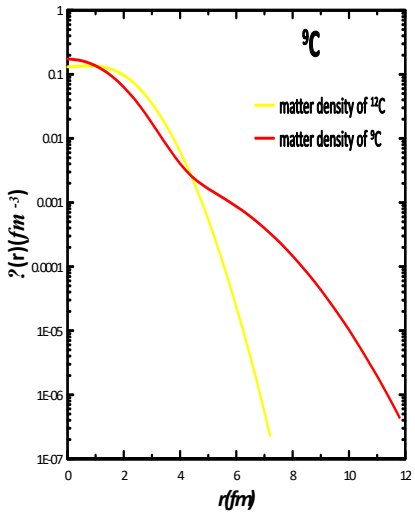

Figure 6. Calculated matter density distribution of proton –rich (^{9}C) with that of stable nuclei (^{12}C)

Figure (5) shows the relation between 2BNDD's (in fm^{-3}) of the ground state and r (in *fm*) With including short range effect (r_c= 0.5 *fm*) and tensor force effect (α =0.1) for ^{9}C nuclei. The blue curve represents 2BNDD's for the core ^{7}Be (proton + neutron) with oscillator size parameter (b_c=1.7 *fm*). The green curve represents 2BNDD's for valence (two proton) for ^{9}C nuclei with oscillator size parameter (b_v=3.47 *fm*), while red solid curve represents the total calculation for the core nucleons and the two valance protons, and the shaded curve represents the experimental [24], we have a long tail that agrees well with the experimental results.

Figure (6) illustrates a calculated matter density distributions of proton-rich ^{9}C (red line) with the matter density distributions of the stable nuclei ^{12}C (yellow line) by using 2BCDD's, we shown along tail is clearly in the matter distribution of the halo nuclei.

The neutron (blue curve), proton (brown curve), and matter (red curve) show densities of ^{9}C we show in Figure (7). It is observed that the proton *rms* radius is more than the neutron *rms* radius, that the proton diffuseness is greater than the neutron diffuseness in ^{9}C, and that there is a significant density differential between the proton and neutron in ^{9}C. The typical behavior of the halo nucleus (the long tail) is clearly seen in the two proton for ^{9}C distributions (brown curve), as shown in these figure. We note that the difference between the radii of the neutron and the proton is (r_p -r_n = 0.42288 *fm*) for ^{9}C. This difference is also supported by the halo structure for these alien cores.

Figure (8) presents the electron form factor for ^{9}C with FC'S using PWBA. Where the average radii of nuclei (b=1.78*fm*) were used, these values were adopted by comparing $\langle r^2 \rangle_{\exp}^{1/2}$ with $\langle r^2 \rangle_{the}^{1/2}$ we get a match with the experimental data. The blue curve represents the form factor of 2BCDD's with finite nucleon size corrected and center of mass correction (F_{fs}(q) ≠0, $F_{cm}(q)$ ≠0), the red curve represents the form factor of 2BCDD's with (F_{fs}(q)= 0, $F_{cm}(q)$ =0), and the circle-packed are experimental data for stable nuclei ^{7}Be [27]. It is clear that the form factor is dependent

on the detailed properties of the two proton halo and the difference in which depends on the mass number and the size parameter b_m ,obtain good form factors at the momentum for q<3.6 *fm* and we note that the behavior of the theoretical results for halo nuclei (^{9}C) matches the practical results for stable nuclei (^{12}C).

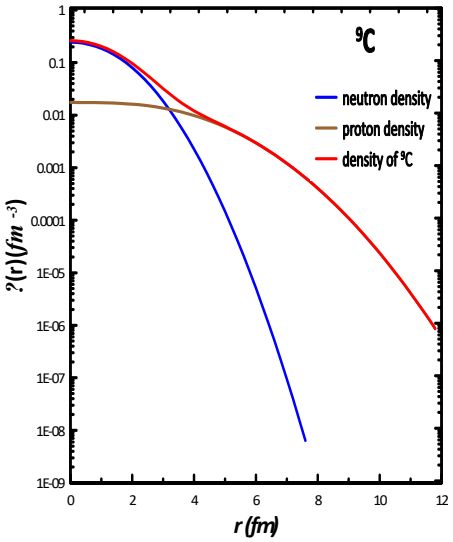

Figure 7. Proton, neutron, and matter densities were calculated for ^{9}C halo nuclei

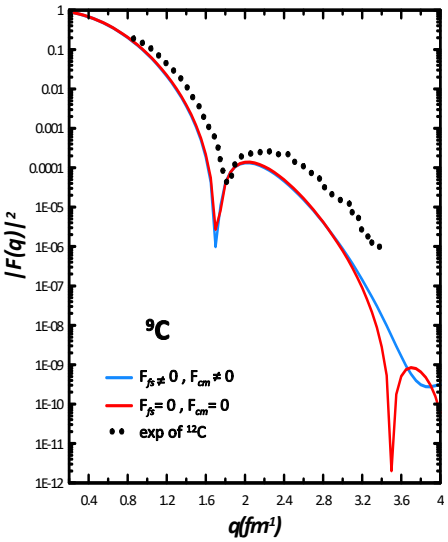

Figure 8. Elastic scattering electron form factor for ^{9}C with experimental data [27]

4. CONCLUSIONS

The measured matter density for our exotic nuclei using the framework of two body nucleon density distribution with effects of tensor force and short range with two different oscillator size parameters *bc* and *bv* showed a long tail behavior. The calculated proton and neutron distributions, density of matter and *rms* radii, are based on the halo nuclei ^{26}F and ^{9}C. The charge density distributions are joined with the PWBA to studied the form factors for these nuclei. The considerable difference in charge form factors between unstable nuclei (^{26}F and ^{9}C) and their stable isotopes (^{19}F and ^{12}C) is attributable to an increase in proton concentrations in the peripheral area.

ORCID IDs

Abeer A.M. Hussein, https://orcid.org/0000-0003-0068-1347; **Ghaith N. Flaiyh,** https://orcid.org/0000-0001-9918-4484

REFERENCES

[1] M. Hongo, and D. Thanh Son ,"Universal Properties of Weakly Bound Two-Neutron Halo Nuclei", Phys. Rev. Lett. **128**, 212501 (2022). https://doi.org/10.1103/PhysRevLett.128.212501

[2] A.N. Antonov, P.E. Hodgson, and I.Zh. Petkov, *Nucleon Momentum and Density Distributions in Nuclei*, (Clarendon Press, Oxford, 1988), pp. 97-102.

[3] I. Tanihata, H. Savajols, and R. Kanungo, "Recent experimental progress in nuclear halo structure studies", Progress in Particle and Nuclear Physics, **68**, 215–313 (2013).

[4] H. Bethe, B.H. Brandow, and A.G. Petschek, "Reference spectrum method for nuclear matter", Phys. Rev. **129**(1), 225-264 (1963). https://doi.org/10.1103/PhysRev.129.225

[5] G.E. Brown, and T.T.S. Kuo, "Structure of finite nuclei and the free nucleon-nucleon interaction", Nucl. Phys. A, **92**(3), 481-494 (1967). https://doi.org/10.1016/0375-9474(67)90627-6

[6] F. Dellagiacoma, G. Orlandiniand, and M. Traini, "Dynamical correlations in finite nuclei: A simple method to study tensor effects", Nucl. Phys. A, **393**(1), 95-108 (1983). https://doi.org/10.1016/0375-9474(83)90066-0

[7] I. Tanihata. J. Phys. G: Nucl. Part. Phys. **22**, 157 (1996). https://doi.org/10.1088/0954-3899/22/2/004

[8] P.G. Hansen, A.S. Jensen, and B. Jonson, Ann. Rev. Nucl. Part. Sci. **45**, 591 (1995). https://www.annualreviews.org/doi/pdf/10.1146/annurev.ns.45.120195.003111

[9] G.M. Sallh, and A.N. Abdullah, Iraqi Journal of Science, **62**(8), 2555-2564 (2021). https://doi.org/10.24996/ijs.2021.62.8.8

[10] Arkan R. Ridha, Wasan Z. Majeed, Iraqi Journal of Science, **63**(3), 977-987 (2022). https://doi.org/10.24996/ijs.2022.63.3.7

[11] B.Q. Chen, Z.Y. Ma, F. Grümmer, and S. Krewald, "Relativistic mean-field theory study of proton halos in the 2s1d shell", J. Phys. G: Nucl. Part. Phys. **24**, 97 (1998). https://doi.org/10.1088/0954-3899/24/1/013

[12] Z. Ren, A. Faessler, and A. Bobyk, "Relativistic mean-field description of a proton halo in the first excited (1/2)+ state of 17F", Phys. Rev. C, **57**, 2752 (1998). https://doi.org/10.1103/PhysRevC.57.2752

[13] A.K. Hamoudi, G.N. Flaiyh, and A.N. Abdullah, "Study of Density Distributions, Elastic Electron Scattering form factors and reaction cross sections of ^{9}C, ^{12}N and ^{23}Al exotic nuclei", Iraqi Journal of Science, **56**(1A), 147-161 (2015). https://www.iasj.net/iasj/download/e5ff2f1a46127a57

[14] K.P. Anjali, K. Prathapan, and R.K. Biju, Braz. J. Phys. **50**, 298 (2020). https://doi.org/10.1007/s13538-020-00750-1

[15] A.N. Antonov, P.E. Hodgson, and I.Zh. Petkov, "Nucleon Momentum and Density Distribution in Nuclei", Z. Physik A, **297**, 257–260 (1980). https://doi.org/10.1007/BF01892806

[16] R.D. Lawson, *Theory of the Nuclear Shell Model*, (Clarendon Press, Oxford, 1980).
[17] A.K. Hamoudi, R.A. Radhi, G.N. Flaiyh, and F.I. Shrrad, "The effect of two body Correlations on the charge density distributions and elastic electron scattering form factors for some 2s-1d shell nuclei", Journal of Al-Nahrain University, **13**, 88-984 (2010). https://www.iasj.net/iasj/download/d9ae0c35e9ff9031.
[18] J. Fiasi, A. Hamoudi, J.M. Irvine, and F. Yazici, J. Phys. G: Nucl. Phys. **4**, 27 (1988). https://doi.org/10.1088/0305-4616/14/1/007
[19] S. Sugimoto, K. Lkeda, and H. Toki, "Study of the effect of the tensor correlation on the alpha-alpha interaction in 8Be with charge and parity projected Hartree-Fock method", Nucl. Phys. A, **789**, 155-163 (2007). https://doi.org/10.1016/j.nuclphysa.2007.04.004
[20] T.T.S. Kuo, and G.E. Brown, "Structure of finite nuclei and the free nucleon-nucleon interaction: An application to ^{18}O and ^{18}F". Nucl. Phys. A, **85**, 40-86 (1966). https://doi.org/10.1016/0029-5582(66)90131-3
[21] A.N. Abdullah, Int. J. Mod. Phys. E, **29**, 2050015 (2020). https://doi.org/10.1142/S0218301320500159
[22] J.D. Walecka, *Electron Scattering for Nuclear and Nucleon Structure*, (Cambridge University Press, Cambridge, 2001), pp. 3112.
[23] A. Ozawa, T. Suzuki, and I. Tanihata, "Nuclear size and related topics", Nucl. Phys. A, **693**, 32–62 (2001). https://doi.org/10.1016/S0375-9474(01)01152-6
[24] S. Ahmad, A.A. Usmani, and Z.A. Khan, Phys. Rev. C, **96**, 064602 (2017). https://doi.org/10.1103/PhysRevC.96.064602
[25] R.E. Warner, F. Carstoiu, J.A. Brown, F.D. Becchetti, D.A. Roberts, B. Davids, M. Horoi, et al, "Reaction and proton-removal cross sections of ^{6}Li, ^{7}Be, ^{10}B, ^{9,10,11}C, ^{12}N, ^{13,15}O, and ^{17}Ne on Si at 15 to 53 MeV/nucleon", Phys. Rev. C, **74**, 014605 (2006). https://doi.org/10.1103/PhysRevC.74.014605
[26] G. Audi, F.G. Kondev, M. Wang, W.J. Huang, and S. Naimi, Chin. Phys. C, **41**, 030001 (2017). https://doi.org/10.1088/1674-1137/41/3/030001
[27] H. Rui, L. Jia-Xing, Y. Jian-Ming, J. Juan-Xia, W. Jian-Song, H. Qiang, Chain. Phys. Lett. **27**(9), 092101 (2010). https://doi.org/10.1088/0256-307X/27/9/092101
[28] H. De Vries, C.W. Jager, and C. De Vries, "Nuclear charge-density-distribution parameters from elastic electron scattering", Atomic Data and Nuclear Data Tables, **36**(3), 495-536 (1987). https://doi.org/10.1016/0092-640X(87)90013-1

ТЕОРЕТИЧНЕ ДОСЛІДЖЕННЯ РОЗПОДІЛУ ГУСТИНИ МАТЕРІЇ ТА ФОРМ-ФАКТОРІВ ПРУЖНОГО РОЗСІЮВАННЯ ЕЛЕКТРОНІВ ЕКЗОТИЧНИХ ЯДЕР (^{26}F ТА ^{9}C)

Абір А. М. Хусейн, Гейт Н. Флей

Факультет фізики, Науковий коледж, Багдадський університет, Багдад, Ірак

Розподіл ядерної густини, середньоквадратичних радіусів і форм-фактори пружного розсіювання електронів розраховано для ядер (^{9}C) (ядро +2p) і (^{26}F) (ядро +2n) з двома різними параметрами ядерного потенціалу для (*bc*) і (*bv*), де використовуються кореляції для обох ефектів (тензорної сили і короткодії), і спостерігається поява довгого розширення в розподілах ядерної густини для цих ядер. Fortran 95 використовувався для програмування ядерних властивостей, таких як густина нуклонів (матерії, нейтронів і протонів), форм-факторів пружного розсіювання електронів і середньоквадратичних радіусів. Визначено, що результати обчислень для цих екзотичних ядер досить добре відповідають експериментальним даним.

Ключові слова: *екзотичні ядра; форм-фактор; ядерна щільність (нейтрон, протон, речовина); багатонейтронні ядра, багатопротонні ядра*